arXiv:2011.01862v1 [cond-mat.soft] 3 Nov 2020

Ring polymers on percolation clusters

K. Haydukivska[1,2] and V. Blavatska[1,2]

[1] Institute for Condensed Matter Physics of the National Academy of Sciences of Ukraine, 79011 Lviv, Ukraine

[2] $\mathbb{L}^4$ Collaboration & Doctoral College for the Statistical Physics of Complex Systems, Leipzig-Lorraine-Lviv-Coventry, Europe

Abstract. In the present work, the cyclic polymer chains (rings) in structurally disordered environment (e.g. in the cross-linked polymer gel) are studied exploiting the model of closed self-avoiding walks (SAWs) trajectories on $d = 3$-dimensional percolation clusters. Numerical simulations with an application of pivot algorithm are performed. The estimates for the universal size and shape characteristics such as size ratios, averaged asphericity and prolateness of typical polymer conformation are obtained. Our results quantitatively describe an elongation and increase of anisotropy of ring polymers in disordered environment comparing with the pure solvent.

PACS numbers: 36.20.-r, 67.80.dj, 64.60.ah, 07.05.Tp

Submitted to: *Journal of Physics: Condensed Matter*

1. Introduction

Closed polymer chains (rings) gain significant interest of researchers with the discovery of certain DNA in circular form [1–3]. Under appropriate synthesis conditions, the covalent linking of the the ends of flexible linear chains (ring formation) is observed during polymerization and polycondensation [4–6]. The statistical properties of circular polymers in dilute solutions have been intensively studied both analytically [7–22] and experimentally [6, 23].

In statistical description of long flexible polymers in solvents one can distinguish a number of conformational properties, which possess universality, i.e. are independent of details of chemical structure, and thus allow to combine the wide range of macromolecules into the so called universality classes. As typical examples, one can consider the averaged radius of gyration $\langle R^2_{g\,\mathrm{chain}}\rangle$ and the end-to-end distance $\langle R^2_{e\,\mathrm{chain}}\rangle$ of linear polymer chains, obeying the scaling law with number of monomers N [24, 25]:

$$\langle R^2_{g\,\mathrm{chain}}\rangle \sim \langle R^2_{e\,\mathrm{chain}}\rangle \sim N^{2\nu}, \tag{1}$$

where $\langle(\ldots)\rangle$ means averaging over an ensemble of possible conformations of macromolecule and ν is universal critical exponent, depending on the space dimension d. In particular, a nice approximation is given by Flory formula [24]: $\nu(d) = 3/(d+2)$,

	g	p	$\overline{\langle A_3 \rangle}$	$\overline{\langle P \rangle}$
pure	0.536(7) [12]	3.217(20) [12]	0.262(1) [12]	0.205(2) [12]
	0.539(25) [10]		0.255(10) [8]	0.151(14) [8]
	0.516 [33]			
	0.53(3) [23]			
our study	0.537(1)	3.288(3)	0.258(1)	0.198(1)
pc, our study	0.548(2)	3.463(6)	0.264(1)	0.201(1)

Table 1. Size ratios and shape parameters of ring polymers in $d = 3$ in pure environment and on the percolation cluster.

which restores the fact that at space dimension above the upper critical one $d_{\rm up}$=4 one has an ideal Gaussian polymer with $\nu(d \geq 4)$=1/2 (apart from logarithmic corrections to scaling). The value of critical exponent ν in 1 is not influenced by changing the topology of polymer structure, and thus the radius of gyration $\langle R^2_{g\,\rm ring}\rangle$ of closed polymer rings obeys exactly the same scaling law [26–28]. Thus, the useful parameter to compare the size measures of linear and ring polymers of the same molecular weight N have been introduced [29]:

$$g \equiv \frac{\langle R^2_{g\,\rm ring}\rangle}{\langle R^2_{g\,\rm chain}\rangle}, \tag{2}$$

which is in turn universal and N-independent quantity. In the case of idealized Gaussian case one has $g = 1/2$ [29], whereas presence of excluded volume effect leads to an increase of this value (see Table 1). Note that for the closed circular polymers, the spanning radius $R_{1/2\,\rm ring}$ is of interest instead of the usual end-to-end distance, and a ratio

$$p \equiv \frac{\langle R^2_{1/2\,\rm ring}\rangle}{\langle R^2_{g\,\rm ring}\rangle} \tag{3}$$

is introduced. For a Gaussian polymer one has $p = 3$, and this ratio again increases when excluded volume is taken into account [27].

To characterize the shape properties of typical polymer chain conformation, the rotationally invariant universal quantities, such as the averaged asphericity $\langle A_d\rangle$ and prolateness $\langle P\rangle$ have been introduced [30, 31]. $\langle A_d\rangle$ takes on a maximum value of one for a completely stretched, rod-like configuration, and equals zero for spherical form, thus obeying the inequality: $0 \leq \langle A_d\rangle \leq 1$. Prolateness $\langle P\rangle$ is positive for prolate ellipsoid-like configurations, and is negative for oblate shapes, being bounded to the interval $-1/4 \leq \langle P\rangle \leq 2$. For a Gaussian ring, an exact value for asphericity parameter is obtained $\langle A_d\rangle = (d+2)/(5d+2)$ [32] . The values of $\langle A_d\rangle$ and $\langle P\rangle$ for ring polymers with excluded volume effect are given in Table 1.

The model of self-avoiding walk (SAW) on a regular lattice was proven to be very successful in in capturing the universal configurational properties of flexible polymers in good solvent [25]. The ring polymer can thus be straightforwardly modeled as a closed SAW trajectory, where the first and the last steps coincide. This model have

been exploited in numerous numerical studies of circular polymers [7–10] and allows to obtain the reliable quantitative estimates for their size and shape properties.

There are numerous physical situations, in which the ring polymers are placed in an structurally disordered environment, e.g. the cross-linked polymer gel in processes of gel electrophoresis [34], colloidal solutions [35], intra- and extracellular environments [36] which are highly crowded due to the presence of a large amount of various biochemical species [37]. An important question is how the universal conformational properties of macromolecules are modified in presence of structural obstacles (impurities) in the system. Within the frames of lattice model of polymers, a disordered medium can be modeled as a randomly diluted lattice, where only a given concentration p of randomly chosen lattice sites allowed for SAWs, whereas the remaining $1-p$ sites containing point-like obstacles. Mostly interesting is the case, when concentration p equals the threshold value p_c (in $d = 3$, in the case of site percolation it reads $p_c = 0.31160$ [38]) and an incipient percolation cluster can be found in the system [39]. The complicated fractal structure of percolation cluster captures the effect of density fluctuations of structural defects, which often lead a considerable spatial inhomogeneity and create pore spaces of fractal structure [40]. In particular, it can be used in modeling the gel structure, which is highly irregular and contain multiple dangling ends [41], which is a distinctive feature of percolation cluster.

Numerous analytical and numerical studies [42–48] quantitatively confirmed the extension of effective size and an increase of anisotropy of typical linear polymer chain conformations on percolation cluster. It is important to note, that complex fractal

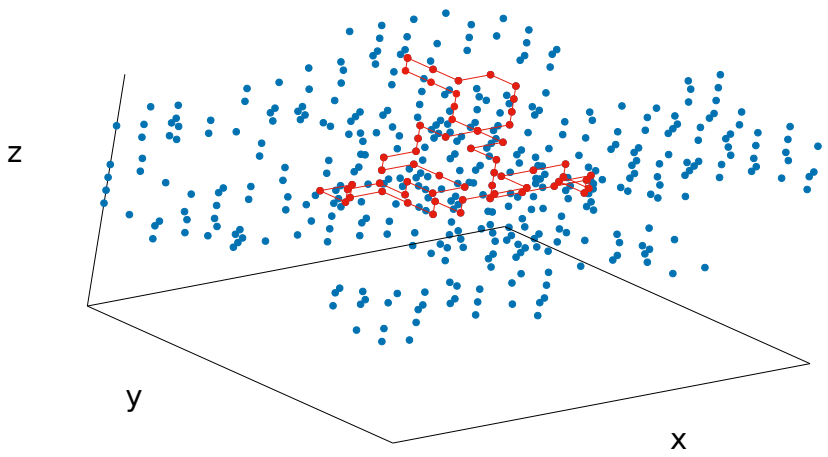


Figure 1. (Color online): The part of percolation cluster constructed on cubic lattice and closed SAW trajectory, allowed to take its steps only on sites belonging to percolation cluster.

structure of underlying percolation cluster causes the change of universality class of SAWs residing on it. In particular, the scaling law (1) holds in this case with larger value of critical exponent $\nu_{p_c}(d = 3) = 0.667(3)$ [47], and asphericity and prolateness values considerably increase comparing with the case of pure lattice [48]. However, though the statistical properties of circular polymers in diluted environments have been considered in numerical simulations [49–51], the thorough study of universal size and shape characteristics of this polymer topology on percolation cluster have not been performed so far and is the aim of the present study.

The layout of the paper is as follows. In the next Section, we short describe the methods of constructing of underlying percolation cluster on cubic lattice and pivot algorithm, used for simulating SAW. The Section 3 contain our main simulation results on size and shape characteristics of closed SAW on percolation cluster. Conclusions are given in Section 4.

2. The method

2.1. Construction of the percolation cluster

We consider site percolation on a regular 3-dimensional lattice of edge length $L = 100$. Each site of the lattice is considered to be empty with probability $p_c = 0.31160$, and containing a point-like obstacle otherwise. To extract the percolation cluster, we apply an algorithm developed by Hoshen and Kopelman [52]. As a first step, a label is prescribed to each empty site in increasing order. At the second step, for each of the labeled site (say, i), we check whether its nearest neighbors are also empty. If the label of the neighbor is larger than that of site i, we change the label of the neighbor to that of site i. Otherwise, we change the label of site i to that of the neighbor. Such an algorithm is applied until no more changes of site labels are needed. As a result, we obtain the groups of clusters of empty sites of different sizes, where all the sites in a given group have the same label. Finally, we check for the existence of a cluster, that wraps around the lattice. If it exists, we have found the percolation cluster. If not, this disordered lattice is rejected and a new one is constructed. A total number $C = 1400$ clusters have been constructed.

2.2. Pivot Algorithm

To study the SAWs having their steps only on the sites belonging to percolation cluster (see Fig. 1), we apply the pivot algorithm, proposed in Ref. [53] and further developed in Refs. [54,55] among others. At a first step, an initial configuration of SAW trajectory of a given length N is build. The SAW is considered to be closed when a walker of N steps returns to the starting point. Then, the sequence of elementary pivot moves, i.e. a lattice symmetry operations (rotation or reflection) are applied to parts of a trajectory. When dealing with open chains, we choose a random point on this trajectory so that it is split into two parts. Then a randomly chosen symmetry operation is applied to

one of the parts. The result of this operation is accepted if the resulting walk is also a self-avoiding and all its steps are on the sites belonging to percolation cluster. If not, the initial configuration is considered one more time. Then a new point is chosen and the procedure is repeated P-times. When dealing with closed trajectories, one more step has to be added in algorithm to ensure that the resulting configuration is also closed. For each of the symmetry operations there always is a plane or an axis of symmetry associated with it and a second point on the closed SAW trajectory that also belongs to that plane or axis (see fig. 2) can be chosen, so that pivot step can be performed between two points.

We consider both open and closed SAW trajectories with the lengths up to $N = 40$ and perform up to $P = 20000$ and $P = 10000$ pivot steps correspondingly. The lower amount of pivot steps for closed SAWs is considered because there is a smaller amount of configurations available comparing with the open case. This procedure is performed on all percolation clusters constructed, taking into account up to 30 different starting configurations on each cluster.

The estimates for any observable O is obtained by performing the double averaging: the first one is performed over all SAW configurations on a single percolation cluster

$$\langle O \rangle = \frac{1}{P} \sum_{i=1}^{P} O_i, \tag{4}$$

the second average is carried out over different realizations of disorder, i.e. over all percolation clusters constructed:

$$\overline{\langle O \rangle} = \frac{1}{C} \sum_{j=1}^{C} \langle O \rangle_j. \tag{5}$$

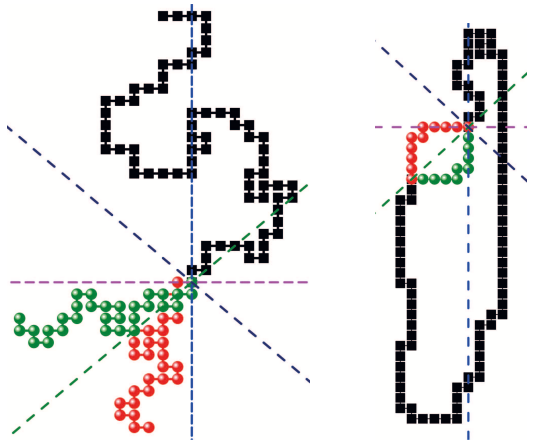


Figure 2. (Color online): Schematic presentation of one of the pivot operations for an open (left) and closed (right) SAW trajectory. Black symbols represent part of the walk that remains intact, red symbols represent parts that get transformed, while green ones depict the results of the transformation. Dash lines show axis of symmetry.

3. Results

To find the estimates for size and shape parameters, we start with evaluation of the components of gyration tensor $\mathbf{Q}$, which in $d = 3$ are given by [30, 31]:

$$Q_{ij} = \frac{1}{N}\sum_{n=1}^{N}(x_n^i - x_{CM}^i)(x_n^j - x_{CM}^j), \quad i,j = 1,\ldots,3, \tag{6}$$

with $\{x_n^1,\ldots,x_n^3\}$ being the set of coordinates of position vector $\vec{R}_n$ of the nth step of SAW trajectory ($n = 1,\ldots,N$) and $x_{CM}^i = \sum_{n=1}^{N} x_n^i/N$ the coordinates of the center-of-mass position vector $\vec{R}_{CM}$. The squared radius of gyration is given by:

$$R_g^2 = \frac{1}{N}\sum_{n=1}^{N}(\vec{R}_n - \vec{R}_{CM})^2 = \sum_{i=1}^{d} Q_{ii} = \mathrm{Tr}\,\mathbf{Q}, \tag{7}$$

whereas asphericity A_d and prolateness P are defined in terms of components of gyration tensor according to [30]:

$$A_3 = \frac{1}{6}\sum_{i=1}^{3}\frac{(\lambda_i - \overline{\lambda})^2}{\overline{\lambda}^2} = \frac{3}{2}\frac{\mathrm{Tr}\,\hat{\mathbf{Q}}^2}{(\mathrm{Tr}\,\mathbf{Q})^2}, \tag{8}$$

$$P = \frac{\prod_{i=1}^{3}(\lambda_i - \overline{\lambda})}{\overline{\lambda}^3} = 27\frac{\det\hat{\mathbf{Q}}}{(\mathrm{Tr}\,\mathbf{Q})^3}, \tag{9}$$

with λ_i being the spread of eigenvalues of gyration tensor, $\overline{\lambda} \equiv \mathrm{Tr}\,\mathbf{Q}/d$ the average eigenvalue and $\hat{\mathbf{Q}} \equiv \mathbf{Q} - \overline{\lambda}\,\mathbf{I}$ (here $\mathbf{I}$ is the unity matrix).

Let us consider the size ratios defined by Eqs. (2) and (3), which allow us to compare the effective extension of closed rings comparing to the linear chains. In Fig. 3 we present our simulation data as functions of trajectory length N. Note, that at small N the size ratio of gyration radii of ring and linear trajectories on percolation cluster $g_{\mathrm{perc}}(N)$ is smaller than that on the pure lattice $g_{\mathrm{pure}}(N)$, whereas it tends to increase faster with N. On the other hand, the ratio of the spanning radii on percolation cluster $p_{\mathrm{perc}}(N)$ is always larger than that on the pure lattice $p_{\mathrm{pure}}(N)$.

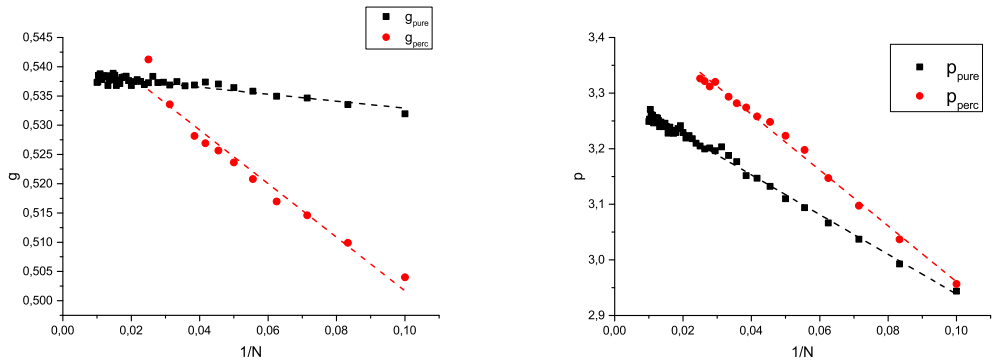


Figure 3. Size ratio (2) on the left and size ratio (3) on the right as functions of $1/N$. Black squares: pure lattice, red circles: percolation cluster.

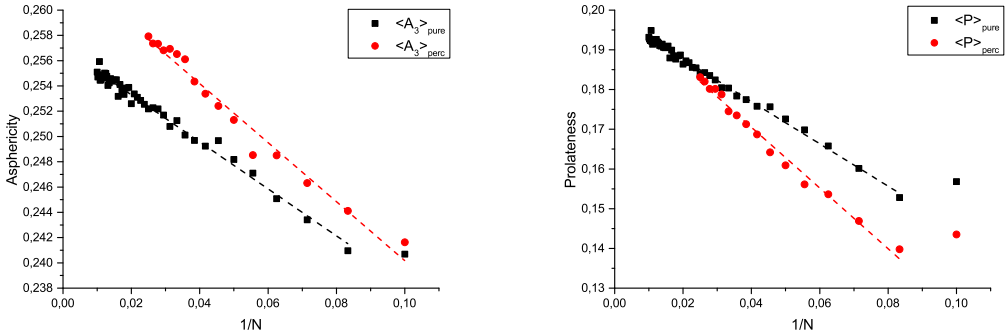


Figure 4. Aspericity on the left and prolateness on the right as functions of $1/N$. Black squares: pure lattice, red circles: percolation cluster.

For finite trajectory lengths N considered in our study, the values of size ratios considerably differ from those for infinitely long structures. The size ratio estimates can be obtained by using a least-square fitting of the form:

$$g_{\rm pure}(N) = g_{\rm pure} + A_1/N, \;\; g_{\rm perc}(N) = g_{\rm perc} + A_2/N, \tag{10}$$

$$p_{\rm pure}(N) = p_{\rm pure} + B_1/N, \;\; p_{\rm perc}(N) = p_{\rm perc} + B_2/N, \tag{11}$$

with A_1, A_2, B_1, B_2 being constants. Results of the approximation are given in table 1. Note that in pure environment our estimates are in good agreement with previous results even though we consider very short trajectories.

Next, we turn our attention to evaluating the set of shape parameters. In Fig. 4 we present our simulation data as functions of length N. The estimates can again be obtained by using a least-square fitting of the form:

$$\langle A_3(N)\rangle_{\rm pure} = \langle A_3\rangle_{\rm pure} + C_1/N, \;\; \overline{\langle A_3(N)\rangle}_{\rm perc} = \overline{\langle A_3\rangle}_{\rm perc} + C_2/N, \tag{12}$$

$$\langle P(N)\rangle_{\rm pure} = \langle P\rangle_{\rm pure} + D_1/N, \;\; \overline{\langle P(N)\rangle}_{\rm perc} = \overline{\langle P\rangle}_{\rm perc} + D_2/N, \tag{13}$$

with C_1, C_2, D_1, D_2 being constants. Results of the approximation are given in table 1. Again our results on pure lattice are in good agreement with previous calculations. The value of prolateness $\overline{\langle P\rangle}_{\rm perc}$ is almost not modified by presence of disorder, whereas asphericity $\overline{\langle A_3\rangle}_{\rm perc}$ is larger as comparing with the case of pure lattice and thus quantitatively describes the increase of asymmetry of typical closed ring trajectory.

4. Conclusions

In the present work we analyzed the conformational properties of closed flexible polymers in disordered environment within the lattice model of SAWs on percolation clusters. The complicated structure of percolation cluster captures in particular the irregular gel structure with the multiple dangling ends [41], and thus the proposed model may describe the situation when the ring polymers are placed in cross-linked polymer gels.

The size and shape properties of a specified polymer conformation are characterized in terms of the gyration tensor $\mathbf{Q}$. The rotationally invariant quantities constructed as combinations of components of $\mathbf{Q}$, such as gyration radius $\langle R_g^2 \rangle$, averaged asphericity $\langle A_3 \rangle$ and prolateness $\langle P \rangle$ are directly obtained in numerical simulations with application of pivot algorithm. All the shape characteristics increase gradually with increasing the length of SAW trajectory. The presence of disorder makes the longer conformations to be more elongated and asymmetric. Our results quantitatively indicate the change of the size and shape parameters of typical closed ring conformations relative to the obstacle-free case.

References

[1] Fiers W and Sinsheimer R L (1962) J Mol Biol **5** 424
[2] Zhou H -X (2003) J Am Chem Soc **125** 9280
[3] Wasserman S A and Cozzarelli N R (1986) Science **232** 951
[4] Brown (Jr) J F and Slusarczuk G M (1965) J Am Chem Soc **87** 931
[5] GeiserG and Hocker H (1980) Macromolecules **13** 653
[6] Roovers J and Toporowski P M (1983) Macromolecules **16** 843 ; Roovers J (1985) J Pol Sci Polym Phys Ed **23** 1117
[7] Bishop M and Michels J P J (1985) J Chem Phys **82** 1059
[8] Bishop M and Michels J P J (1986) J Chem Phys **85** 5961
[9] Bishop M and Michels J P J (1986) J Chem Phys **84** 444
[10] Bishop M and Michels J P J (1988) J Chem Phys **89** 1159
[11] Diehl HW and Eisenriegler E (1989) J Phys A: Math Gen **22** L87
[12] Jagodzinski O Eisenriegler E and Kremer K (1992) J Phys I France **2** 2243
[13] Obukhov SP Rubinstein M and Duke T (1994) Phys Rev Lett **73** 1263
[14] Muller M Wittmer JP and Cates ME (2000) Phys Rev E **61** 4078
[15] Deutsch JM (1999) Phys Rev E **59** R2539
[16] Shimamura M K and Doguchi T (2001) Phys Rev E **64** 020801
[17] Alim K and Frey E (2007) Phys Rev Lett **99** 198102
[18] Bohr M and Heermann D W (2010) J Chem Phys **132** 044904
[19] Calabrese P Pelissetto A and Vicari E (2002) J Chem Phys **116** 8191
[20] Sakauer T (2011) Phys Rev Lett **106** 167802
[21] Jung Y Jeon C Kim J Jeong H Jun S and Ha B -Y (2012) Soft Matter **8** 2095
[22] Rosa A Orlandini E Tubiana L and Micheletti C (2011) Macromolecules **44** 8668
[23] Higgins J Dodgson K and Semlyen J A (1979) Polymer **20** 553
[24] de Gennes PG *Scaling Concepts in Polymer Physics* (Cornell University Press, Ithaca, 1979)
[25] des Cloizeaux J and Jannink G *Polymers in Solutions: Their Modelling and Structure* (Clarendon Press, Oxford, 1990)
[26] Duplantier B (1994) Nucl Phys B **430** 489
[27] Prentis J J (1982) J Chem Phys **76** 1574
[28] Privman V and Rudnick J (1985) J Phys A: Math Gen **18** L789
[29] Zimm B H and Stockmeyer W H (1949) J Chem Phys **17** 1301
[30] Aronovitz J A and Nelson D R (1986) J Physique **47** 1445
[31] Rudnick J and Gaspari G (1986) J Phys A **19** L191 ; Gaspari G Rudnick J and Beldjenna A (1987) J Phys A **20** 3393
[32] Gaspar iG Rudnick J and Beldjenna A (1987) J Phys A: Math Gen **20** 3393
[33] Douglas J F and Freed K F (1984) Macromolecules **17** 2344
[34] Dorfman K D (2010) Rev Mod Phys **82** 2903

[35] Pusey P N and van Megen W (1986) Nature **320** 340
[36] Kumar S and Li M S (2010) Phys Rep **486** 1
[37] Minton A (2001) J Biol Chem **276** 10577
[38] Grassberger P (1992) J Phys A **25** 5867
[39] Stauffer D and Aharony A [**?**]ntroduction to Percolation Theory (Taylor and Francis London 1992)
[40] Dullen A L *Porous Media: Fluid Transport and Pore Structure* (Academic New York 1979)
[41] Whytock S and Finch J (1991) Biopolymers **31** 1025
[42] Woo KY and Lee S B (1991) Phys Rev A **44** 999 ; Lee S B (1996) J Korean Phys Soc **29** 1; Nakanishi H and Lee S B (1991) J Phys A **24** 1355 ; Lee S B and Nakanishi H (1988) Phys Rev Lett **61** 2022
[43] Grassberger P (1993) J Phys A **26** 1023
[44] Rintoul M D Moon J and Nakanishi H (1994) Phys Rev E **49** 2790
[45] Ordemann A Porto M and Roman H E (2002) Phys Rev E **65** 021107; (2002) J Phys A **35** 8029
[46] Janssen H-K and Stenull O (2007) Phys Rev E **75** 020801(R)
[47] Blavatska V and Janke W (2008) J Phys A: Math Gen **42** 015001
[48] Blavatska V and Janke W (2010) J Chem Phys **133** 184903
[49] Gersappe D and De La Cruz M O (1994) Moleciilar Simulation **13** 267
[50] Kuriata A and Sikorski A (2015) CMST **21** 21
[51] Michieletto D Baiesi M Orlandini E and Turner M S (2014) Soft Matter **11**
[52] Hoshen J and Kopelman R (1976) Phys Rev E **14** 3438
[53] Lal M (1969) Molec Phys **17** 57
[54] Madras N and Sokal A D (1988) J Stat Phys **50** 109
[55] Clisby N (2010) J Stat Phys **140** 349